Research paper

Continuous inline mapping of a dissolved methane plume at a blowout site in the Central North Sea UK using a membrane inlet mass spectrometer – Water column stratification impedes immediate methane release into the atmosphere

CrossMark

Stefan Sommer*, Mark Schmidt, Peter Linke

GEOMAR Helmholtz Centre for Ocean Research Kiel, Wischhofstr. 1-3, 24148 Kiel, Germany

A B S T R A C T

The dissolved methane (CH_4) plume rising from the crater of the blowout well 22/4b in the Central North Sea was mapped during stratified water column conditions. Geochemical surveys were conducted close to the seafloor at 80.3 m water depth, below the thermocline (61.1 m), and in the mixed surface layer (13.2 m) using membrane inlet mass spectrometry (MIMS) in combination with a towed CTD. Seawater was continuously transferred from the respective depth levels of the CTD to the MIMS by using an inline submersible pump. Close to the seafloor a well-defined CH_4 plume extended from the bubble release site ~460 m towards the southwest. Along this distance CH_4 concentrations decreased from a maximum of 7872 nmol l^{-1} to less than 250 nmol l^{-1}. Below the thermocline the well-defined CH_4 plume shape encountered at the seafloor was distorted and filaments were observed that extended towards the west and southwest in relation to current direction. Where the core of the bubble plume intersected this depth layer, footprints of high CH_4 concentrations of up to 17,900 nmol l^{-1} were observed. In the mixed surface layer the CH_4 distribution with a maximum of up to 3654 nmol l^{-1} was confined to a small patch of ~60 m in diameter. The determination of the water column CH_4 inventories revealed that CH_4 transfer across the thermocline was strongly impeded as only ~3% of the total water column inventory was located in the mixed surface layer. Best estimate of the CH_4 seabed release from the blowout was 1751 tons yr^{-1}. The fate of the trapped CH_4 (~97%) that does not immediately reach the atmosphere remains speculative. In wintertime, when the water column becomes well mixed as well as during storm events newly released CH_4 and the trapped CH_4 pool can be transported rapidly to the sea surface and emitted into the atmosphere.

1. Introduction

In November 1990, a shallow gas pocket in the Central North Sea (well 22/4b) UK was accidently drilled by Mobile North LTD that resulted in a severe gas blowout. Although the gas flow strongly decreased directly after the event, vigorous methane (CH_4) bubble ebullition still continues until today and has been observed to emanate from a 60 m wide crater (Schneider von Deimling et al., 2007; this volume). During a survey in May 1994 that was conducted across the North Sea, CH_4 concentrations of up to 1453 nmol L^{-1} were recorded at the sea surface close to the

blowout (Rehder et al., 1998) resulting in high fluxes of the prominent greenhouse gas into the atmosphere. Public awareness of this blowout ceased until the event of the Deepwater Horizon oil spill in April 2010 in the Gulf of Mexico, leading to a need for the novel assessment of the risks and the environmental hazards involved in marine oil and gas exploration.

Yet, to date except studies in this volume (Leifer and Judd, in this issue) almost no attempts have been made to quantify blowout discharge rates of CH_4 from the seafloor, nor to determine the distribution of the dissolved CH_4 plume in the water column or to assess the CH_4 release into the atmosphere. Here, we report on the spatial distribution of the dissolved CH_4 plume in the close surrounding of the blowout that was measured on three different depth levels at a high spatial resolution to constrain the water column CH_4 inventory using quasi-continuous membrane inlet mass

spectrometry (MIMS). The measurements were conducted during stratified water column conditions where vertical density gradient suppresses turbulent diffusive transport (Linke et al., 2010; Leifer et al., in this issue; Schneider von Deimling et al., in this issue) leading to trapping of a fraction of the gas released from the seafloor below and within the thermocline (Schneider von Deimling et al., 2011; Leifer et al., in this issue).

2. Methodology

2.1. Working area

The blowout site (well 22/4b) is located in the UK EEZ at 57°55′18″N and 1°37′52″E in the Central North Sea, for details of bathymetry see Schneider von Deimling et al. (2007; in this issue). At this site, vigorous gas bubble release takes place that originates from an aquifer at the base of the Quaternary strata (Rehder et al., 1998; Leifer and Judd, in this issue). Gas is released from a 60 m wide crater that is formed within the 96 m deep sea floor, for the detailed description of this site as well as its history since the blowout event in November 1990 see Schneider von Deimling et al. (in this issue; 2007). In situ sampling of gas bubbles at 118 m water depth revealed the emanating gas represents 88–90% vol CH_4 that is of biogenic origin (Schneider von Deimling et al., in this issue). The bubble release creates a jet towards the surface with a rising velocity of about 50 cm s^{-1} (Schneider von Deimling et al., in this issue; Wilson et al., in this issue). The core of the bubble stream is surrounded by bubbles, which instead of rising in a straight vertical line have been observed to exhibit spiral vortical motions during their rise (Schneider von Deimling et al., in this issue). Observations using the two-manned submersible JAGO during RV Alkor cruise AL290 in 2006 revealed strong up- and downward convective currents close to the bubble jet.

2.2. Data acquisition methods

During RV Alkor cruise AL374 (29.05.-11.06.2011; Linke et al., 2011) the distribution of dissolved CH_4 in the near field of the bubble plume (534 × 667 m) and it's transfer through the water column to the mixed surface layer, where it eventually enters the atmosphere, was studied during stratified water column conditions (Fig. 1, CTD#8 at 93 m water depth; Pos.: 57°55.448′ N, 1°38.052' E). The distribution of dissolved CH_4 was mapped using a MIMS (see section 2.4) in combination with a video controlled water sampling rosette equipped with a CTD (SBE9plus) that was towed across the blow out area (Fig. 2, for the tracks see Fig. 6A-C). Similar to the approach of Mächler et al. (2012), an underwater pump (DRE 100/2/G50V, AGB Pumpen, Hamburg, Germany), typically used for rural sewage treatment, generated a continuous water stream through a hose from the CTD to the laboratory, where quasi-continuous inline MIMS gas measurements were made (for details see below). The towing speed of this CTD system ranged between 0.5 and 0.8 kt s. GPS position was logged parallel to the CTD data from an external GPS device, which was mounted close to the CTD winch. A digital video telemetry system (Sea and Sun Trappenkamp, Germany; Linke et al., 2015) allowed safe deployment and towing of the CTD system very close to the sea floor.

In total, three video-guided CTD tracks were conducted in the near-field of the bubble stream (Table 1). CTD track # 10 (09.06.2011) was performed close to the seafloor at an average water depth of 80.3 m (Fig. 6C). CTD track # 11 (10.06.2011) took place below the thermocline at a water depth of 61.1 m (Fig. 6B). The third CTD track (#12, 10.06.2011) was carried out in the mixed

surface layer at 13.2 m water depth to assess potential methane release into the atmosphere (Fig. 6A).

The deployments were conducted during a tidal phase covering predominantly either SW or NE current directions. The sampling rate of the MIMS was 0.2 Hz. The actual response time and time needed to recover from high CH_4 concentrations of e.g. up to 8430 nM was determined using single distinct peaks beyond background, indicating a reaction time of <20 s and a 95% recovery time of <60 s. During post-processing the sampling time of the MIMS data was back-calculated to the sampling time of the CTD system, which concurrently to the physical data further received the NMEA position signal of an external GPS allowing for geo-referencing of the CTD-as well as of the MIMS data. The time period between water sampling at the inlet of the CTD and its arrival at the membrane inlet in the laboratory was ~2 min; this was considered during spatial analysis of the methane data. The 2D contour plots of the CH_4 levels for each survey were constructed applying the kriging gridding procedure using the Surfer Version 9 software (Golden Software Inc.). The 3D CH_4 distribution (see supplemental material S1) was determined applying inverse distance (isotropic) gridding of longitude, latitude and water depth as well as trilinear CH_4 concentration interpolation for volume rendering using Voxler 3.3 (Golden Software Inc.).

Supplementary data related to this article can be found online at http://dx.doi.org/10.1016/j.marpetgeo.2015.08.020.

2.3. Current measurements

The tidal regime, i.e. pressure, as well as the magnitude and velocity of currents at the blowout site were measured during the time period 7.06.2011, 20:00 to 9.09.2011 17:30 UTC using a small Satellite Lander STL3 (Flögel et al., 2013) equipped with an upward looking 307.2 kHz ADCP (RDI-Teledyne Instruments) and a SBE16 plus V2 CTD. The STL3 was placed directly in the crater of the blow out (Position: 57°55.360′ N, 1°37.862′ E) in a water depth of 104 m. For the time period 3.06.2011, 07:00 until 6.06.2011 14:00 UTC this system (STL1) has been further deployed in a distance of
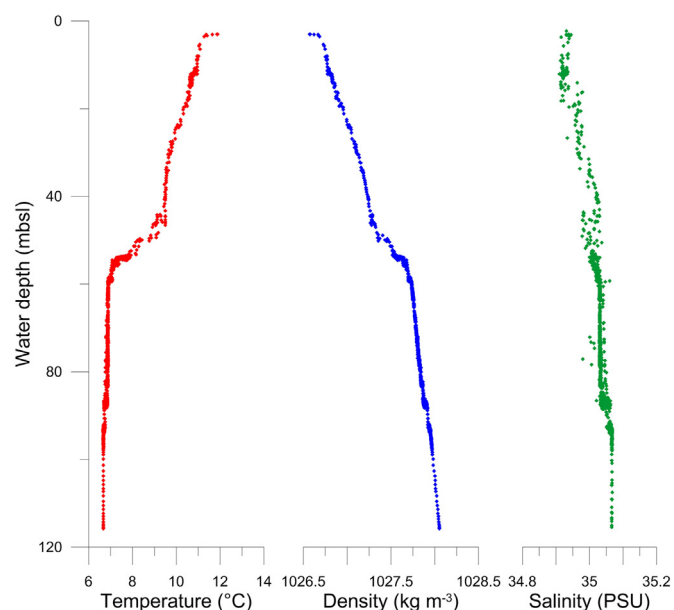

Fig. 1. Water column physical properties during deployment of CTD #8 at 93 m water depth; Pos.: 57°55.448′ N, 1°38.052′ E.
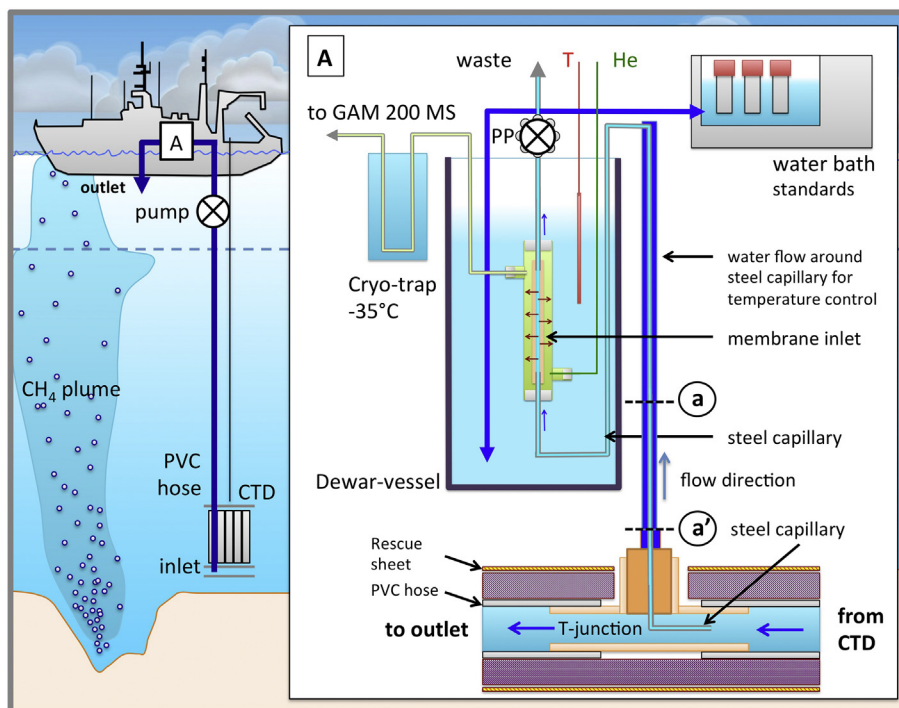
Fig. 2. Set up of methane measurement combining inline membrane inlet mass spectrometry and a towed video CTD. Water was pumped to the shipboard laboratory using a pump which was submersed in about 10–15 m water depth. Within the laboratory this water stream was subsampled and transferred to the membrane inlet for gas extraction. Care was taken to reduce temperature changes from the sampling point at the CTD until gas extraction in the inlet. The connection of water sample flow between the subsampling site and just prior to the inlet is indicated by a and a'. For details see text.

Table 1
Details of the CTD surveys #10 (09.06.11), #11 (10.06.11) and #12 (10.06.11) conducted around the blowout. The start and end time (UTC) denotes the time period used for the construction of the spatial CH_4 distribution shown in Fig. 6A–C. Due to the vertical movements of the CTD during towing, average depth ± standard deviation is given.

CTD track	Avg. depth (m)	Start (UTC)	End (UTC)	Duration (h)	No. of CH_4 measurements	Area covered (km^2)	Tidal regime
10	80.3 ± 4.2	07:29	10:30	3.0	2171	0.37	High to low, SW
11	61.1 ± 2.8	09:35	11:35	2.0	1444	0.72	High to low, SW
12	13.2 ± 0.5	12:44	17:02	4.3	3103	0.73	Low to high, NE

about 29 nm from the blowout in the Sleipner oil field in a water depth of 83 m (Position: 58°22.446′ N, 1°55.976′ E; 79 m water depth).

2.4. Continuous in line gas measurements using a membrane inlet mass spectrometer

Dissolved CH_4 was measured ex situ using a membrane inlet quadrupole mass spectrometer (GAM 200, InProcessInstruments, Bremen) whose gas extraction inlet was inline with the water stream that was continuously pumped to the laboratory through a 100 m long PVC hose (i.d.: 2.5 cm, wall thickness 4.5 mm, Fig. 2). The entrance of the hose was mounted on the CTD frame beneath the Niskin bottles. The underwater pump (denoted as pump in Fig. 2) yielded a flow rate of 31.9 L min^{-1} as determined by measuring the time until a defined volume of 10 L was filled and was clamped onto the CTD wire at a water depth of about 10–15 m. Although, some submersible pumps cause cavitation, which would result in bubble formation, this was not observed.

The hose on deck and throughout its way to the laboratory was insulated thermally by using a foamed plastic mantle and additionally, by wrapping into rescue cover sheets to reduce temperature changes. Water temperature at the hose inlet (CTD) and the hose outlet outside on deck (denoted as outlet in Fig. 2) differed by ~0.2 °C.

Plastic material is not entirely gas-tight hence diffusion of CH_4 across the hose wall might occur. The wall thickness of the PVC hose was 4.5 mm; hence, according to the Einstein–Smoluchovski relation (t = L^2/2D, t: elapsed time, L: diffusion length, D: diffusion constant) the time needed for CH_4 to diffuse through the tube wall amounts to 598 h (D$_{CH4}$ in plasticized PVC: 0.047 × 10^{-10} m^2 s^{-1} at 25 °C; Kjeldsen, 1993). Hence, CH_4 diffusion across the wall in relation to high flow velocity of 31.9 l min^{-1} (i.e. 65 m min^{-1}) can be neglected. The water flow in the hose can lead to temporal blurring of variations and carry over effects that can affect the gas measurements. However, given the high fluid flow velocity, the boundary at the hose wall can be assumed thin reducing these effects. In addition, sub-sampling from the hose using a steel capillary was conducted at its centre where the free flow velocity

was highest (Fig. 2 panel A), which furthermore suppresses such carry over effects. This is also indicated by the fast recovery time as mentioned before.

Lastly, flow rate variability of the submersed pump might affect slightly the measured CH_4 distribution. The flow rate variability of the pump is unknown but cannot be excluded. Hence, in order to estimate the effect of variable flow rates of the submersed pump on the spatial distribution of CH_4 we assumed a 5% variability of the flow rate (± 1.6 L min^{-1}). This would correspond to a delay or early arrival of the water-front moving through the hose to the site, where subsampling was conducted using a steel capillary (i.e. after ~100 m, for details see below and Fig. 2) of ± 4.6 s. At a maximum towing speed of 0.8 kn this results in a variability in the moved distance of ± 1.9 m. With a meridional extension of the investigation area of about 440 m this corresponds to an uncertainty of $\pm 0.4\%$ in the location of a gas measurement. We are aware that bubble entrainment might have occurred, which might have led to increased CH_4 concentrations directly within the plume but not in the remaining area.

Subsampling of water from the PVC hose (Fig. 2, panel A) took place in the laboratory by using a steel capillary (i.d. 1.1 mm) that was connected to the glass membrane inlet. The distance between the location of subsampling and the membrane inlet was about 150 cm. Along this distance the steel capillary was permanently cooled to the respective in situ temperature of the subsea hose inlet. To achieve the best possible temperature stability, the membrane inlet itself was kept submersed in a water bath using a Dewar vessel. This arrangement was placed in a cooler. During the deployments the temperature of the inlet increased by a maximum of 0.2 °C. Constant flow of the subsampled water through the membrane inlet was achieved using a peristaltic pump (Ismatec; denoted as PP in Fig. 2) generating a flow rate of 3.5 ml min^{-1}. The design of the glass membrane inlet followed that of G. Lavik (Max Planck Institute for Marine Microbiology, Bremen, Fig. 2). Within the glass inlet the water was sucked through a permeable silicone tube (Dow Corning, Cat. No. 508-007, length 40 mm, i. d. 1.57 mm, o. d. 2.41 mm). The wall thickness of the silicone tube was 0.42 mm, time needed for CH_4 to diffuse across the tube wall amounts to 4 s (D_{CH4} in silicone: 221×10^{-10} m^2 s^{-1} at 25 °C; Kjeldsen, 1993). Gas flow from the inlet to the quadrupole mass spectrometer was conducted in a steel capillary supported with Helium that was supplied through a fused silica capillary (i.d. 100 μm, see Fig. 2, green line). The distance between the inlet and the ion source of the quadrupole was about 80 cm. An in-line cryo-trap (−35 °C, ethanol) between the inlet and the mass spectrometer was used to reduce water vapour. Concentrations of CH_4 were obtained from calibrated ion currents at the mass to charge ratio of 15. A Secondary Electron Multiplier was used as a detector. Ion currents of CH_4 were calibrated using aqueous CH_4 standards of 1.8, 9.8, 100, 1,000, and 10,000 ppm. For each calibration these standards were produced by equilibrating pre-filtered (0.2 μm) seawater (80 ml) in a 100 ml flask with respective standard gases at the in situ temperature for 30 min in a water bath (Fig. 2, panel A). System response to these standards (9.8, 100, 1,000, 10,000 ppm) was linear. Laboratory tests confirmed that the time period of 30 min is sufficient to reach equilibrium (Walther, 2013). The CH_4 detection limit of the MIMS is about 20 nmol L^{-1}. MIMS derived methane concentrations were cross-validated with concentrations that were measured in discrete water samples that were taken during the different pump CTD tracks by Niskin bottles (Fig. 3). Seawater from Niskin bottles was transferred into pre-evacuated glass bottles and dissolved gases were extracted according to Keir et al. (2008). The methane concentration of extracted gas samples were determined onboard RV Alkor by using a "Thermo Trace ultra" gas chromatograph (equipped

with FID, RTX1-60 m capillary column, Ø = 0.53 mm, N$_2$ carrier gas).

3. Results and discussion

3.1. Bubble release and transport

Vigorous gas bubble release from the sea floor was recorded hydro-acoustically using a 38 kHz shipboard echosounder (Fig. 4), but was also observed visually during the video-guided CTD surveys as well as during a dive with JAGO during RV Alkor cruise AL290 in 2006 (Schneider von Deimling et al., in this issue). During slack water conditions the bubble flare was observed in the sonar extending to about 65 m and penetrated into the thermocline that extended from about 60 to 40 m (Figs. 1 and 4). The diameter of the bubble stream was about 10–20 m at the crater rim (Schneider von Deimling et al., in this issue). The direction of the bubble plume distinctively changed with current strength and current direction.

The current recordings during the STL3 deployment in the crater of the blow out were strongly disturbed by the reflections of the gas bubbles as noted in Nauw et al. (in this issue) and Wiggins et al. (in this issue). Hence, the current regime was taken from the STL1 deployment that was conducted 3 days before at the Sleipner area. Since the seafloor topography between the two ADCP sites is rather smooth and there is no profound change in water depth, this slightly remote site can be used for this approach. Additionally at both sites the same tidal regime is present. Between the tides at the 29 nm remote site and the blowout site there is only a slight time difference as the tides propagates from the north towards the south. The changes of the current direction and velocity showed a strong tidal component with SW and NE as major directions (Fig. 5). For the CTD survey #11 the major current directions were shown in Fig. 6B as trajectories of the movement of a water parcel starting at the blowout position. These trajectories were derived calculating the distance a hypothetical water parcel would have moved in the time interval of 85.6 s between each subsequent ADCP velocity and direction measurement and summing up these vectors over a time period for 1 h.
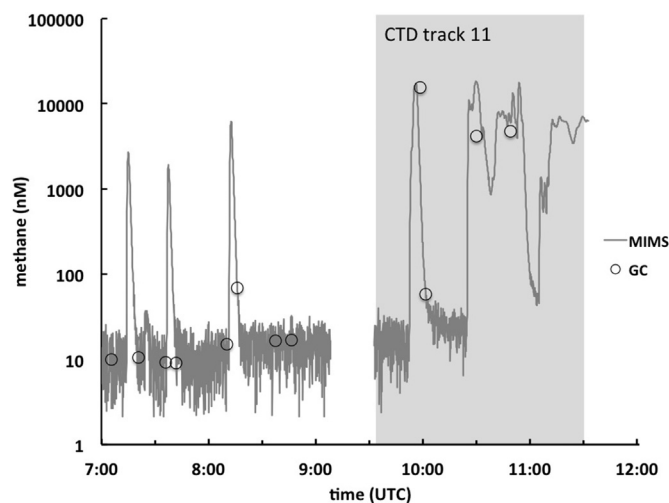

Fig. 3. Comparison between MIMS based and standard gas chromatographical CH_4 measurements during CTD track #11. The time span underlain by grey area was used to construct the contour plot shown in Fig. 6B.
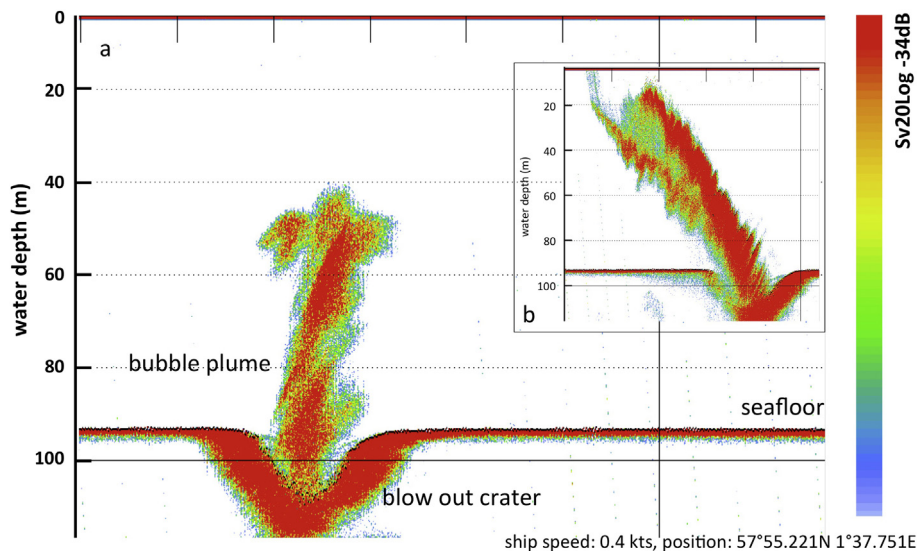
Fig. 4. A, Gas flare at the blowout site well 22/4b recorded with the shipboard 38 kHz echosounder. Insert b shows the gas flare almost reaching to the sea surface.
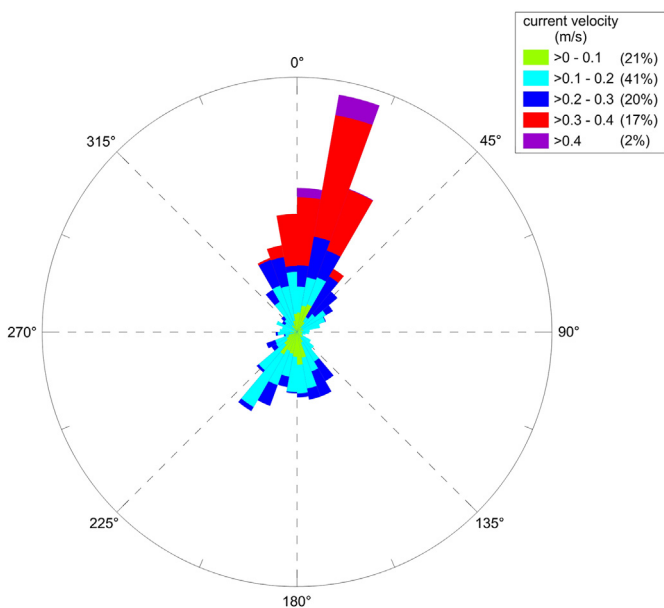

Fig. 5. Major current directions recorded during the Satellite Lander deployment STL1 from the 3.06.2011, 07:00 until 6.06.2011 14:00 UTC in a distance of about 29 nm from the blowout in the Sleipner oil field. The percentages denote the relative abundance of the respective current velocities.

3.2. High-resolution spatial dissolved CH_4 distribution at the blowout site

The CTD surveys with quasi-continuous online MIMS measurements allowed fast mapping of the dissolved CH_4 plume at the blowout at very high spatial resolution, which by no means can be achieved during conventional CTD water sampling casts. Although such mass spectrometric offshore gas detection techniques are still scarce in the literature, prominent examples such as the use of an underwater membrane inlet mass spectrometer for the tracking of hydrocarbon plumes exist, for instance the determination of subsea methane plumes after the Deepwater Horizon oil spill (Camilli et al., 2010), localization of seafloor petroleum contamination (Camilli et al., 2009), or studying naturally occurring oil and gas seeps off California (Valentine et al., 2010). These examples highlight the enormous potential of mass spectrometry for identifying subsea hydrocarbon seepage (leakage) and monitoring the distribution of hydrocarbon plumes in the water column in general.

At 80 m water depth, only a few meters above seafloor (CTD survey #10), a well-defined dissolved CH_4 plume could be monitored that extended from the blowout crater, indicated by a white circle in Fig. 6C, to about 460 m towards southwest. Along this distance, the CH_4 concentration was diluted from a maximum CH_4 concentration of 7872 nmol L^{-1} to less than 250 nmol L^{-1}. Shortly after the start of the monitoring survey, the bubble plume was encountered transecting the 80-m depth horizon in a direction of 235° and in a distance of ∼50 m from the injection point leaving a footprint of strongly elevated CH_4 levels (Fig. 6C).

Although the CTD survey #11 below the thermocline encompassed a similar tidal regime compared to CTD survey #10 (Table 1), the well-defined CH_4 plume shape encountered during CTD survey #10 was not observed but instead was much more distorted and characterized with the occurrence of filaments extending towards west and southwest (Fig. 6B). The lateral extension of elevated CH_4 concentrations was not fully covered during this survey. The vertical eddy-diffusive transport of solutes in a stratified water column is strongly impeded, whereas the lateral transport of dissolved gases is enhanced due to the absence of horizontal density gradients (McGinnis et al., 2004; Linke et al., 2010; Schneider von Deimling et al., 2011). Hence, with increasing distance to the bubble stream the thermocline represents an effective barrier for dissolved constituents. During bubble plume experiments in a stratified lake it has been shown that the core of the plume itself is highly turbulent and well-mixed with regard to the distribution of temperature and oxygen (McGinnis et al., 2004). The near-field is highly complex with multiple detrainments occurring at various water depths due to lateral advective cross flow (Leifer et al., 2009). Similarly to this observation, during the CTD survey #11 a strong lateral SW current, which is indicated by the ADCP data, probably induced the formation of filaments of elevated CH_4 levels to spread out along isopycnals. This also is indicated by the superimposed current trajectories shown in Fig. 6B. The spatial spread
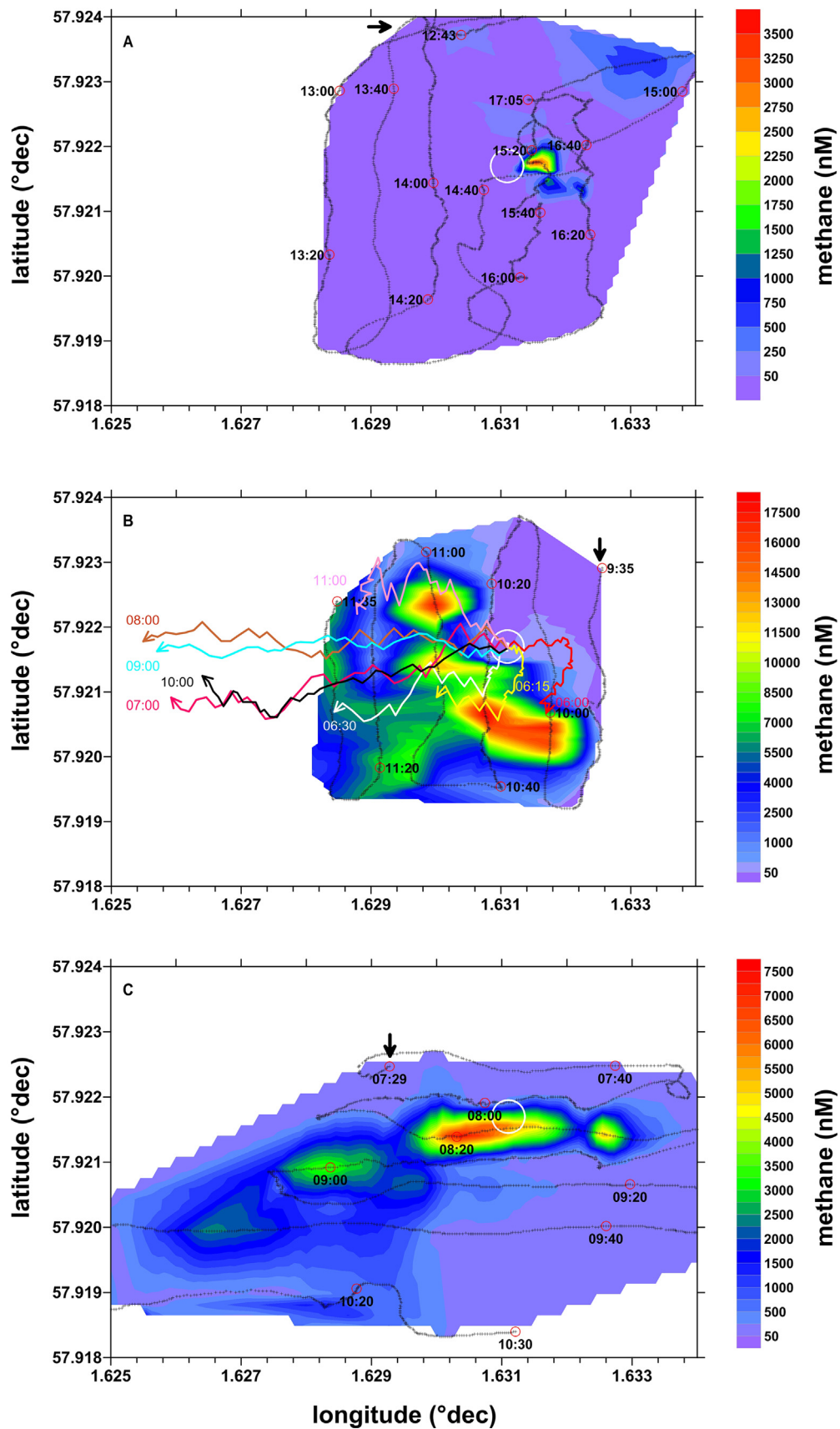
Fig. 6. A–C: Dissolved methane plume measured during the CTD surveys #10 at 80.3 m (panel C), #11 at 61.1 m (panel B) and #12 at 13.2 m water depth (panel A). The tracks of the surveys and the positions where measurements were obtained are indicated (black crosses). The white circle indicates the position of the blowout crater at the seafloor. The red circles denote the position of the CTD at a certain time. The black arrows indicate the location of the start of the different surveys. Flow trajectories are provided for survey #11, the times provide the start time of each trajectory. (For interpretation of the references to colour in this figure legend, the reader is referred to the web version of this article.)
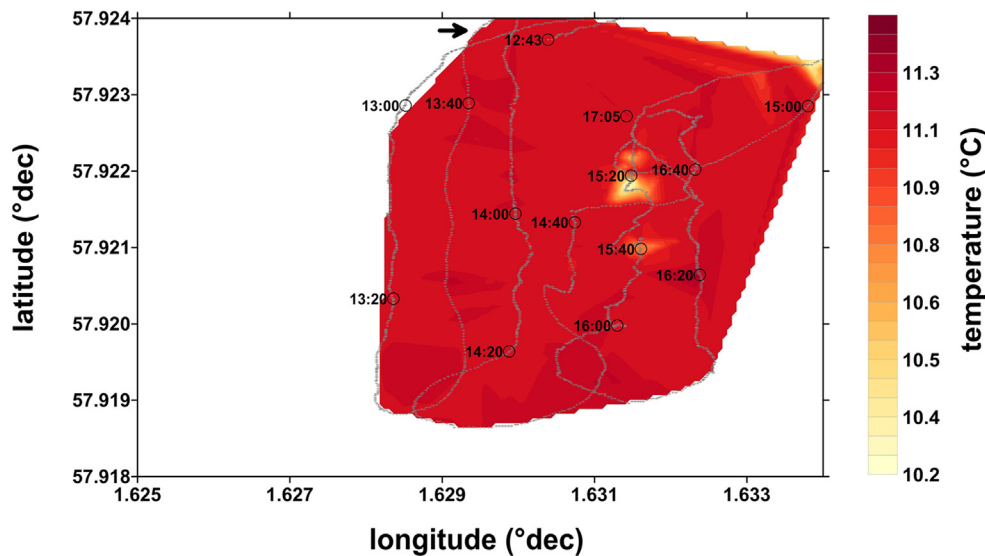
Fig. 7. Temperature measured during CTD survey #12 at 13.2 m water depth. The tracks of the survey and the positions where measurements were obtained are indicated (grey crosses). The red circles denote the position of the CTD at a certain time. The black arrow indicates the location of the start of the surveys. (For interpretation of the references to colour in this figure legend, the reader is referred to the web version of this article.)

of the dissolved CH_4 plume further nicely correlates with hydroacoustical observations that clearly indicate lateral extrusions of the bubble plume below the thermocline (Schneider et al., in this issue; Wilson et al., in this issue).

In comparison to CTD survey #10 much higher CH_4 concentration maxima of around 17,300, 12,900 and 17,900 nmol L^{-1} could be determined during CTD survey #11. The concentration maxima were measured in patches of about 100–160 m in diameter, which were located in southwestern, western, and northwestern directions at distances of about 100–140 m from the blowout crater. As already reasoned above, it seems that these patches were caused by the bubble plume interaction with the 61 m water depth layer, leaving a footprint of strongly elevated methane concentrations when it rotates with changing current direction from south at the beginning of the survey to northwest towards the end of the survey. Interestingly, the diameter of these patches is only slightly bigger than that determined for the 80 m layer survey confirming the laboratory- and field observations of an almost non-expanding bubble core (McDougall, 1978; McGinnis et al., 2004) as well as field observations that were made about the shape of the bubble plume of the investigated blowout (Schneider von Deimling et al., in this issue).

The CTD survey #12 in the well mixed surface layer at 13 m water depth revealed elevated dissolved CH_4 concentrations of up to 3654 nmol L^{-1} confined to a well-defined spot of about 60 m in diameter in close proximity of the gas bubble injection point

(Fig. 6A). This is astonishing, since similarly to the CTD surveys #10 and #11, this survey #12 also comprised changes in the current direction, hence, a more blurred CH_4 distribution would have been expected. It appears, that only at locations where the bubble stream is breaking through the thermocline and reached the mixed surface layer, elevated levels of dissolved CH_4 can be measured. Indeed, this was shown by the coincidence of enhanced CH_4 levels with colder temperatures compared to average temperatures measured at this depth level (Fig. 7). As has been suggested by several plume models (McGinnis et al., 2004, and references therein) and a plume description (Schneider von Deimling et al., in this issue), colder bottom water must have been entrained at the base of the bubble plume and transported by it to this depth horizon and eventually to the sea surface (Fig. 7), as reported in the CTD data in Leifer et al. (in this issue), too. It is however required that this upward advection is compensated by a downward directed flow (Schneider von Deimling et al., in this issue; Wilson et al., in this issue). Upward transport of cold water was not detected during CTD survey #11, which was likely due to the very low temperature difference of ~0.1 °C between the water body at 61 m and the bottom water at about 80 m (Fig. 1). There might have been the possibility to observe the downward flow of warmer water from within the thermocline into the colder water body at 61 m as downward jets reported by Wilson et al. (in this issue). However, temperature changes measured during CTD survey #11 are mainly controlled by vertical uplift of the towed CTD into the thermo-

Table 2
Methane inventories calculated for the different CTD surveys.

CTD track	Avg. depth(m)	Grid cell area/no. Grid cells[a] $(m^2)/n$	Area of excess CH_4[b] (km^2)	CH_4 inventory[c] (kg)	CH_4 inventory (for 1 km^2) (kg)
10	80.3	98.0/2178	0.21	0.25	1.2
11	61.1	75.6/2571	0.19	1.45	7.8
12	13.2	79.4/608	0.05	0.02	0.5

[a] Number of grid cells with CH_4 levels >50 nmol L^{-1}.
[b] Area where CH_4 levels >50 nmol L^{-1} were measured.
[c] CH_4 inventory determined for the area of excess CH_4.

cline, which was caused by variable towing speed of the research vessel.

Questions might arise to what extent the CH_4 distributions shown in Fig. 6A–C represent the actual state at the time of the survey rather than superimposed over previous CH_4 inventories. Fig. 6A–C depict the dissolved methane distribution at the time of the measurement including the effects of transport, mixing and consumption i.e. by microbial methane oxidation. Since consumption is relatively slow the presented distribution is mainly governed by transport. Hence great care has been taken to conduct these measurements within one tidal phase (i.e. one current regime) (cf. Fig. 5). Our measurements (Figs. 3, 6A–C) further indicate that between the two subsequent current regimes when the plume is directed either in SW or NE direction very little if any CH_4 remained in the water column from the previous tidal phase, which could contribute to the actual measurements.

3.3. From depth level specific CH_4 inventories towards an estimate of the total CH_4 mass flux

Vertical mass flux of CH_4 via bubble ebullition and bubble plumes has been assessed using transport/dissolution models in combination with field data (e.g. Leifer and Patro, 2002; McGinnis and Little, 2002; McGinnis et al., 2004; Linke et al., 2010). Further attempts were made by directly measuring bubble ebullition using video footage from which bubble characteristics such as size and rise velocity can be determined (Leifer et al., in this issue; Schneider von Deimling et al., in this issue).

In an approach similar to that of Heeschen et al. (2005) and Mau et al. (2006), we used the measured dissolved CH_4 inventories of the investigated depth layers (Fig. 6A-C) to extrapolate the total water column CH_4 inventory and combine this with an best estimate of the time needed to build up this inventory in order to obtain a conservative estimate of the fraction of dissolved CH_4 mass release from the blowout site.

The CH_4 inventories of the different CTD surveys at 80.3, 61.1, and 13.2 m water depth were calculated using the grid that was generated to construct the contour plots depicted in Fig. 6A–C. Due to the detection limit of the MIMS of ~20 nmol L^{-1} and in order to consider potential carry over effects only CH_4 concentrations assigned to the respective grid cell in excess to 50 nmol L^{-1} were considered. The cell inventory was calculated by multiplying the CH_4 concentration assigned during the gridding procedure to each cell with the respective grid cell area for a layer thickness of 10 cm (Table 2). Subsequently, the CH_4 inventories for the survey at 80.3, 61.1 and 13.2 m water depth were calculated by summing up the respective cell inventories, which amount to 0.25, 1.45, and 0.02 kg CH_4 respectively.

As discussed above, the thermocline acts as a barrier preventing elevated dissolved CH_4 mass flux to the mixed surface layer. To account for this during the extrapolation of the total water column inventory, the water column was subdivided into the three depth zones, the zone below the thermocline (BTC, 80.3 to 61.1 m), the

thermocline (TC, 61.0 to 40 m) and the well-mixed surface layer (MSL, 39.9 to the surface). The total inventories of the zone below and within the thermocline were extrapolated assuming a linear relationship between the CH_4 inventories determined during the three different CTD surveys. This approach accounts for detrainments of CH_4 rich water not only to occur at the base of the thermocline but also at various depths as indicated by field measurements and the bubble plume model of McGinnis et al. (2004). Water depths deeper than 80.3 m to the seafloor and the volume of the crater of the blow out were not considered due to a lack of appropriate CH_4 data allowing the calculation of the inventory. Within the mixed surface layer density gradients can be neglected, hence the CH_4 distribution measured at the 13.2 m depth horizon was assumed to be uniform throughout this layer. This is also indicated by the studies of Schneider von Deimling et al. (in this issue) and Leifer et al. (in this issue), which based on hydro-acoustics report the formation of a well-confined secondary bubble plume at this depth zone. A bubble plume forms when gas is vigorously released from the seabed. When this plume reaches the thermocline only the largest bubbles avoid detrainment and continue as a secondary plume with a momentum high enough to overcome this barrier and reach the sea surface (McDougall, 1978). The inventories determined for the BTC, TC and MSL indicate that CH_4 transfer across the thermocline is indeed strongly impeded as only ~3% of the total water column inventory is located in the mixed surface layer (Table 3).

The methane mass release from the blowout was approached by assessing the time needed to build up the calculated dissolved CH_4 inventories, which beside physico-chemical properties of the plume is depending on current velocity and direction. This approach assumes that at least between each subsequent ebb tide phase the dissolved CH_4 inventory from the previous phase was completely renewed due to horizontal advection as is indicated in Fig. 6A–C. According to the duration of the surveys #10 and #11, which both present spatially clearly defined dissolved CH_4 distributions with no apparent effects of CH_4 carry over from the previous phases time periods of 3 and 2 h, respectively (see Table 1), were assumed as maximum time periods needed for the formation of the respective dissolved CH_4 inventories. Due to the irregular track covering a much longer time period than would be actually needed to map the small patch of dissolved CH_4 in the MSL 1 h was arbitrarily assumed for CTD survey #12.

We are aware that our estimate of the seabed CH_4 release from the blowout of 1247 tons yr^{-1} in 2011 involves simplifications and uncertainties. But nevertheless it supplements other attempts to further constrain the CH_4 release from the blowout site using a completely different methodology. As generally the aerobic microbial CH_4 oxidation is viewed as being quite slow (Reeburgh, 2007 and references therein) microbial CH_4 removal during the short time periods of the different surveys has been neglected in the estimate. Our approach further assumes that the CH_4 in the bubbles becomes fully dissolved until it reaches the sea surface. How-

Table 3
Water column CH_4 inventories extrapolated for the zone below the thermocline (BTC), the thermocline (TC) and the mixed surface layer (MSL). The release rates were determined based on the time needed to build up the inventories in the different depth zones, for details see text. The CO_2 equivalent was calculated assuming a global warming potential (GWP) of CH_4 for 100 yr period of 25 (Shindell et al., 2009).

Depth zone	CH_4 inventory (tons)	CH_4 release (tons yr^{-1})	CO_2 equivalent[b] (mio tons yr^{-1})
BTC	0.16	714	0.015
TC	0.15	452	0.009
MSL	0.01	80[a]	0.002
total	0.32	1247	0.030

[a] A build up time of 1 h instead of the actual time period of 4.3 h was used for survey #12.

[b] The GWP is defined as the integrated global mean radiative forcing out to a selected time of an emission pulse of 1 kg CH_4 relative to that for 1 kg CO_2 (Shindell et al., 2009).

ever, gas measurements of bubbles reaching the sea surface revealed that they still contained ~25% CH_4 (Schneider von Deimling et al., in this issue). Yet, these authors report that a major part of the rising bubbles was trapped in the thermocline and a secondary plume is formed in the mixed surface layer. This plume is characterized with a relatively low bubble transport to the sea surface so that only about 2% of the methane released at the seafloor is emitted into the atmosphere, justifying the above assumption. Another major uncertainty represents the time needed to build up the inventories at the different depth levels, which particularly for the inventory in the mixed surface layer was difficult to constrain. Given the restricted spatial CH_4 distribution and the overall low CH_4 levels determined during the CTD survey #12, an even 4 times shorter time interval (15 min) would increase the total CH_4 release by 19% to 1488 tons yr^{-1}. In the gas bubble plume Schneider von Deimling et al. (in this issue) report the formation of micro methane gas bubbles with diameters less than 200 μm. Apparently, they became trapped below the thermocline and probably rapidly swept away by currents. Hence, a fraction of the methane is exported to the far field of the gas plume, which was not entirely covered during this study. Especially during CTD survey #11 the entire dissolved CH_4 plume was not mapped completely and the depth zones below 80.3 m and inside the crater was not considered. Assuming an 25% higher inventory for depth level 61.1 m, the overall CH_4 release increases by another 15% to about 1751 tons yr^{-1}. This estimate corresponds to a CH_4 release of ~78 L s^{-1} under atmospheric pressure, which is about 9 fold lower than the gas release of 90 L s^{-1} that was determined based on the bubble volume and number of bubbles under in situ pressure (Leifer et al., in this issue). However, dramatic variations in emission strength have been documented for this site (Wiggins et al., in this issue). Assuming a global warming potential of 25 (Shindell et al., 2009), the estimated source strength of the blowout in comparison to other major anthropogenic greenhouse gas sources such as for instance the yearly CO_2 emission caused by the German traffic in 2012 (Umwelt Bundesamt, 2013) is minor, representing only about 0.02% and might be considered negligible. Still, all the different approaches (hydroacoustics, modelling, measurements of the dissolved gas phase, etc.) to determine the source strength of methane release in such a particular setting inherit their uncertainties. Hence, the growing opportunity of combining these methods for cross-validation might contribute to better constrain the actual gas emission in future.

4. Conclusions

Despite the uncertainties involved in the calculation of the CH_4 inventory, it became apparent that a substantial part of ~97% of the dissolved methane originating from the blowout site (well 22/4b) does not immediately reach the atmosphere, but is retained in the water column below and presumably within the thermocline. This corresponds with observations of the structure of the bubble plume made by Schneider von Deimling et al. (in this issue), who estimated that only about 2% of the entire amount of CH_4 injected into the water column is directly entering the atmosphere. The fate of the trapped vast dissolved CH_4 fraction remains speculative. Microbial oxidation in the water column acting on longer time scales as well as the slow transfer of CH_4 across the MSL into the atmosphere also considering methane that has been transported away from the blowout by currents was hypothesized. In wintertime, when the water column becomes well-mixed newly released CH_4 but also the trapped CH_4 pool can be easily transported to the sea surface via turbulent diffusion and emitted into the atmosphere (e.g. Schneider von Deimling et al., 2011). It is even conceivable, that following a quiescent phase during strong storm events, the trapped CH_4 pool might be emptied at once, resulting

in a CH_4 pulse into the atmosphere. These aspects are certainly important and need attention in the environmental impact assessment of the blowout but require a more detailed study of the dissolved CH_4 concentrations in the surrounding of the blowout as well as atmospheric CH_4 measurements during different seasons.

References

Camilli, R., Bingham, B., Reddy, C.M., Nelson, R.K., Duryea, A.N., 2009. Method for rapid localization of seafloor petroleum contamination using concurrent mass spectrometry and acoustic positioning. Mar. Pollut. Bull. http://dx.doi.org/10.1016/j.marpolbul.2009.05.016.

Camilli, R., Reddy, C.M., Yoerger, D.R., Van Mooy, B.A.S., Jakuba, M.V., Kinsey, J.C., McIntyre, C.P., Sylva, S.P., Maloney, J.V., 2010. Tracking hydrocarbon plume transport and biodegradation at deepwater horizon. Science 330, 201–204.

Flögel, S., Pfannkuche, O., Linke, P., Karstensen, J., Dullo, C., 2013. A new stand-alone modular ocean laboratory – MoLab: 100 days in an arctic cold-water coral reef. EMSO Meeting – European Multidisciplinary Seafloor and Water Column Observatory, Rome, 13–15 Nov. 2013, Italy.

Heeschen, K.U., Collier, R.W., de Angelis, M.A., Suess, E., Rehder, G., Linke, P., Klinkhammer, G.P., 2005. Methane sources, distributions, and fluxes from cold vent sites at hydrate ridge, Cascadia Margin. Glob. Biogeochem. Cycl. 19, GB2016. http://dx.doi.org/10.1029/2004GB002266.

Keir, R.S., Schmale, O., Walter, M., Sültenfuß, J., Seifert, R., Rhein, M., 2008. Flux and dispersion of gases from the "Drachenschlund" hydrothermal vent at 8°18'S, 13°30'W. Earth Planet. Sci. Lett. 270, 338–348.

Kjeldsen, P., 1993. Evaluation of gas diffusion through plastic materials used in experimental and sampling equipment. Water Res. 27, 121–131.

Leifer, I., Judd, A., 2015. The UK22/4b blowout 20 years on: investigations of continuing methane emissions from sub-seabed to the atmosphere in a North sea context. J. Mar. Petrol. Geol. (in this issue).

Leifer, I., Patro, R.K., 2002. The bubble mechanism for methane transport from the shallow sea bed to the surface: a review and sensitivity study. Cont. Shelf Res. 22, 2409–2428.

Leifer, I., Jeuthe, H., Gjøsund, S.H., Johansen, V., 2009. Engineered and natural marine seep, bubble-driven buoyancy flows. J. Phys. Oceanogr. 39, 3071–3090.

Leifer, I., Solomon, E., von Deimling, J.S., Rehder, G., Coffin, R., Linke, P., 2015. The fate of bubbles in a large, intense bubble megaplume for stratified and unstratified water: numerical simulations of 22/4b expedition field data. J. Mar. Petrol. Geol. (in this issue).

Linke, P. (Ed.), 2011. RV Alkor Cruise Report 29.05.-14.06.2011, ECO2 Sub-seabed CO_2 Storage: Impact on Marine Ecosystems. IFM-GEOMAR Report Nr. 51, Kiel, ISSN:1614-6298.

Linke, P., Sommer, S., Rovelli, L., McGinnis, D.F., 2010. Physical limitations of dissolved methane fluxes: the role of bottom boundary layer processes. Mar. Geol. 272 (1–4), 209–222. http://dx.doi.org/10.1016/j.margeo.2009.03.020.

Linke, P., Schmidt, M., Rohleder, M., Al-Barakati, A., Al-Farawati, R., 2015. Novel online digital video and high-speed data broadcasting via standard coaxial cable onboard marine operating vessels. J. Mar. Technol. Soc. 49, 7–18.

Mächler, L., Brennwald, M.S., Kipfer, R., 2012. Membrane inlet mass spectrometer for the quasi-continuous on-site analysis of dissolved gases in groundwater. Environ. Sci. Technol. 46, 8288–8296.

Mau, S., Sahling, H., Rehder, G., Suess, E., Linke, P., Soeding, E., 2006. Estimates of methane output from mud extrusions at the erosive convergent margin off Costa Rica. Mar. Geol. 225, 129–144.

McDougall, T., 1978. Bubble plumes in stratified environments. J. Fluid Mech. 85 (4), 655–672.

McGinnis, D.F., Little, J.C., 2002. Predicting diffused-bubble oxygen transfer rate using the discrete-bubble model. Water Res. 36, 4627–4635.

McGinnis, D.F., Lorke, A., Wüest, A., Stöckli, A., Little, J.C., 2004. Interaction between a bubble plume and the near field in a stratified lake. Water Resour. Res. 40. http://dx.doi.org/10.1029/2004WR003038.

Nauw, J., Linke, P., Leifer, I., 2015. Bubble momentum plume as a possible mechanism for an early breakdown of the seasonal stratification in the northern North Sea. J. Mar. Petrol. Geol. (in this issue).

Reeburgh, W.S., 2007. Oceanic methane biogeochemistry. Chem. Rev. 107, 486–513.

Rehder, G., Keir, R.S., Suess, E., Pohlmann, T., 1998. The multiple sources and patterns of methane in North sea waters. Aquat. Geochem 4, 403–427.

Shindell, D.T., Faluvegi, G., Koch, D.M., Schmidt, G.A., Unger, N., Bauer, S.E., 2009. Improved attribution of climate forcing to emissions. Science 326. http://dx.doi.org/10.1126/science.1174760.

Umwelt Bundesamt, 2013. Hintergrund: Treibhausgasausstoss in Deutschland 2012 www.umweltbundesamt.de.

Valentine, D.L., Reddy, C.M., Farwell, C., Hill, T.M., Pizarro, O., Yoerger, D.R., Camilli, R., Nelson, R.K., Peacock, E.E., Bagby, S.C., Clarke, B.A., Roman, C.N., Soloway, M., 2010. Asphalt volcanoes as a potential source of methane to late pleistocene coastal waters. Nat. Geosci. 3. http://dx.doi.org/10.1038/NGEO848.

von Deimling, J.S., Brockhoff, J., Greinert, J., 2007. Flare imaging with multibeam systems: data processing for bubble detection at seeps. Geochem. Geophys. Geosys. 8. http://dx.doi.org/10.1029/2007GC001577.

von Deimling, J.S., Rehder, G., Greinert, J., McGinnis, D.F., Boetius, A., Linke, P., 2011. Quantification of seep-related methane gas emissions at Tommeliten, North Sea. Cont. Shelf Res. 31, 867–878.

von Deimling, J.S., Linke, P., Schmidt, M., Rehder, G., 2015. Ongoing methane discharge at well site 22/4b (North Sea) and discovery of a spiral vortex bubble plume motion. J. Mar. Petrol. Geol. (in this issue).

Walther, S., 2013. Solubility of Methane in NaCl Brines. A Comparative Analytical Study Using Membrane Inlet Mass Spectrometry and Gas Chromatography. University Kiel, Kiel, p. 33.

Wiggins, S.M., Leifer, I., Linke, P., Hildebrand, J.A., 2015. Long-term acoustic monitoring at North Sea well site 22/4b. J. Mar. Petrol. Geol. (in this issue).

Wilson, D., Leifer, I., Maillard, E., 2015. Megaplume bubble process visualization by 3D multibeam sonar mapping. J. Mar. Petrol. Geol. (in this issue).